Dyes and Pigments 81 (2009) 119–123

Contents lists available at ScienceDirect

Dyes and Pigments

journal homepage: www.elsevier.com/locate/dyepig

Photophysical properties of a naphthalimide derivative encapsulated within Si-MCM-41, Ce-MCM-41 and Al-MCM-41

Guodong Chen [a], Lingzhi Wang [a], Jinlong Zhang [a,*], Feng Chen [a], Masakazu Anpo [b]

[a] Laboratory for Advanced Materials, Institute of Fine Chemicals, East China University of Science and Technology, Meilong Road, Shanghai 200237, People's Republic of China
[b] Graduate School of Engineering, Osaka Prefecture University, 1-1 Gakuen-cho, Sakai 599-8531, Japan

ARTICLE INFO

Article history:
Received 15 February 2007
Received in revised form 20 June 2008
Accepted 24 September 2008
Available online 7 October 2008

Keywords:
MCM-41
Naphthalimide derivative
Fluorescence
Photoinduced electron transfer

ABSTRACT

4-Piperazinyl-*N*-methyl-1,8-naphthalimide (PMN) was synthesized and encapsulated into mesoporous molecular sieves. The fluorescent emission spectra and fluorescence decay of PMN/M-MCM-41 (where M = Si, Ce, Al) were used to investigate the photophysical properties of the hybrid composites. The emission intensity of 4-piperazinyl-*N*-methyl-1,8-naphthalimide can be increased by decreasing the pH environment of the hybrid composites; the emission intensity varied with different MCM-41 hosts in the order: PMN/Al-MCM-41 > PMN/Si-MCM-41 > PMN/Ce-MCM-41; the fluorescence lifetime of PMN molecules followed the same order. The reasons for the improved fluorescence intensity and the prolonged lifetime of PMN in a low pH environment and Al-MCM-41 are discussed.

1. Introduction

MCM-41 (Mobile Crystalline Material) is an ordered mesoporous material, that comprises a honeycomb-like structure of uniform mesopores running through a matrix of amorphous silica. The hexagonally arranged uniform pore structure of MCM-41 has attracted much attention owing to its large surface area and narrow pore size distribution. The incorporation of dye molecules into mesoporous molecular sieves leads to organic–inorganic composite materials. Compared with dyes in solution, these functionalized mesoporous materials have many advantages, such as high thermal and mechanical stability and high resistance towards UV radiation. Consequently such hybrid materials enable potential applications in optical sensors [1], optical switches [2], lasers [3], frequency doubling [4] and drug delivery [5,6]. The transition metal and rare earth metal have been introduced into various kinds of mesoporous molecular sieves [7,8]. The dye molecules in such metal-doped molecular sieves are expected to exhibit peculiar photophysical and photochemical properties; electron transfer from the excited dye molecules to the titanium oxide can occur in the channel of Ti-MCM-41 [9]. Zhang et al. [10] found large shifts in fluorescence spectra when C.I. Basic Violet 10 (*Rhodamine B*) was included in Ce-MCM-48, Fe-MCM-48, Cr-MCM-48 than that in Si-MCM-48 and the fluorescent lifetime of the cationic dye within Ce-MCM-48 decreased with increasing cerium content.

Separation of charges is one of the most fundamental processes that have been investigated in numerous chemical and biological systems [11]. Electron donor–electron acceptor molecules serve as an ideal system to mimic natural photosynthetic process. Naphthalimide derivatives comprising an amino moiety as electron donor and 1,8-naphthalimide as electron acceptor have been reported as fluorescent dyes in fluorescent sun collectors, liquid-crystal additives, fluorescent sensors, as well as fluorescent markers in medicine and biology [12]. The work concerns the inclusion of a naphthalimide derivative, 4-piperazinyl-*N*-methyl-1,8-naphthalimide (PMN) as guest molecule within an inorganic matrix. According to the literature [13], PMN molecules are able to recognize protons; photoinduced electron transfer (PET) within PMN molecules is considered as a significant pathway to fluorescence quenching between the fluorophore and the donor. Protonation of the terminal *N* atom will hinder the PET process and thus fluorescence will be regenerated. The effect of the local environment upon fluorescent emission spectra for different kinds of hosts as well as the fluorescence lifetime of the hybrid materials were investigated.

2. Experimental

2.1. Synthesis of 4-piperazinzyl-N-methyl-1,8-naphthalimide

The method used for the synthesis of 4-piperazinzyl-*N*-methyl-1,8-naphthalimide was reported earlier by Gan [13]. The particular synthesis method is depicted as follows.

* Corresponding author. Tel./fax: +86 21 64252062.
E-mail address: jlzhang@ecust.edu.cn (J. Zhang).

0143-7208/$ – see front matter © 2008 Elsevier Ltd. All rights reserved.
doi:10.1016/j.dyepig.2008.09.013

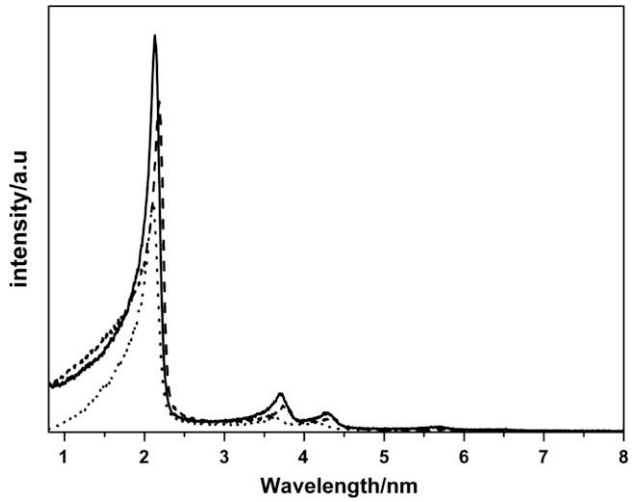

Fig. 1. Low-angle XRD patterns of Si-MCM-41 (solid line), Al-MCM-41 (dotted line), Ce-MCM-41 (dashes line).

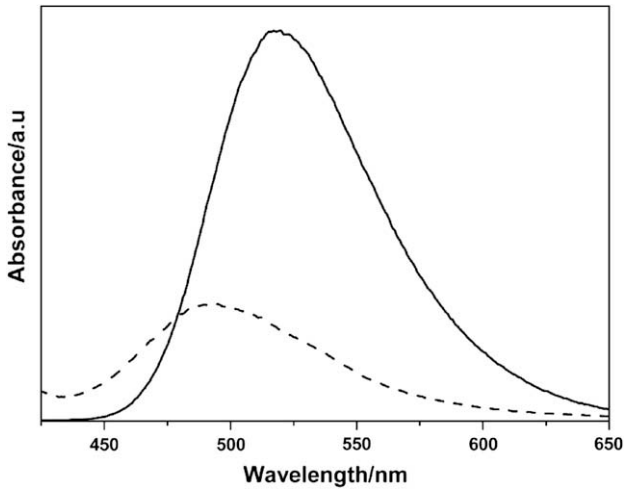

Fig. 3. Fluorescent emission spectra of PMN in methanol/water (v/v = 4:1) solution (10^{-4} M, solid line) and in MCM-41 (dashed line), excited at 396 nm.

4-Bromo-*N*-methyl-1,8-naphthalimide was prepared from 4-bromo-1,8-naphthalic anhydride and methtylamine aqueous solution at ambient temperature for 3 h. The mixture was filtered and washed by ethanol. Crystallization of the solid from chlorobenzene yielded a white solid which can be used without any purification. Mp 185.0–186.5 °C.

A round-bottomed flask, equipped with a magnetic stirrer and a reflux condenser, was charged with 2 g 4-bromo-*N*-methyl-1,8-naphthalimide, 20 ml methyl glycol, 4 g piperazine hexahydrate, and a catalylic amount of triethylamine and stirred for 4 h in an oil bath at 90 °C. The reaction mixture was allowed to cool to ambient temperature and poured into water. Then the crude product was extracted by 80 ml ethyl acetate and the solvent was evaporated. Crystallization of the residue from ethanol and minimum amount of water afforded 4-piperazinzyl-*N*-methyl-1,8-naphthalimide as yellow solid with a yield of 75%. Mp 201–203 °C; literature Mp 200–202 °C. ^{1}H NMR(500 MHz, DMSO-d_6): $\delta = 8.46$ (m, 2H), 8.40 (d, $J = 8.10$ Hz, 1H), 7.80 (t, $J = 7.37$, $J = 8.33$ Hz,1H), 7.31 (d, $J = 8.14$ Hz, 1H), 3.37 (s, 3H, $-CH_3$), 3.14(t, 4H, $-N(CH_2)_2-$), 2.99(t, 4H, $HN(CH_2)_2-$). FT-IR(KBr): 3338.38($HN(CH_2)_2-$), 2823.09, 1691.88(C═O), 1650.04(C═O), 1588.99, 1575.66, 1455.39, 1408.76, 1397.36, 1370.56, 1285.92, 1221.59, 1040.97, 785.00, 756.93 cm^{-1}.

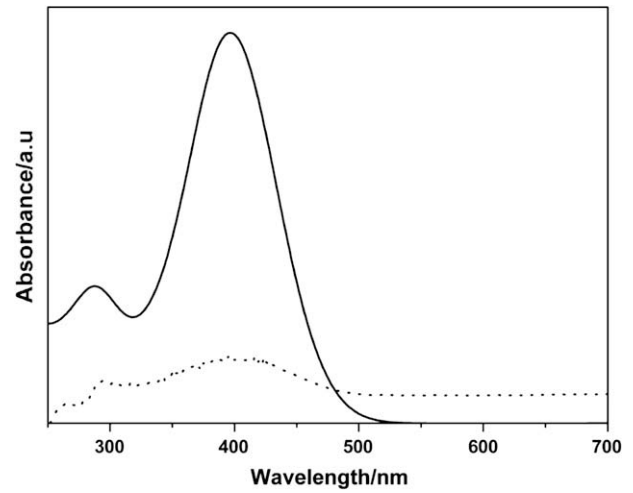

Fig. 2. The absorbance spectra of PMN molecules in Si-MCM-41 (dotted line) and in methanol/water (v/v = 4:1) solution (10^{-4} M, solid line).

Anal. Found: C 68.98, H 5.77, N 14.17; Calc. for $C_{17}H_{17}N_3O_2$: C 69.14, H 5.80, N 14.23.

2.2. Synthesis of Si-MCM-41 and Me-MCM-41 (Me = Ce, Al)

Me-MCM-41 was synthesized by hydrothermal method. In a typical synthesis, 2.4 g cetyltrimethylammonium bromide (CTAB) was dissolved in 36 ml distilled water and 31 ml NH_4OH. 10 ml tetraethylorthosilicate (TEOS) was added to this solution dropwise under stirring, after which, 10 ml metal ion aqueous solution was added to the ensuing gel and the mixture was stirred for 2 h. The molar composition of the final gel mixture was $1SiO_2$:0.01-Me:0.15CTAB:11.6NH_3:89.6H_2O. Finally, the obtained mixture was transferred into Teflon-lined autoclave and heated at 393 K for 48 h. The white solid was filtered, rinsed with large amount of distilled water and dried in air. The as-synthesized MCM-41 was calcined at 543 K for 1 h to remove the physisorbed water and then it was heated at 823 K for 5 h.

The Si-MCM-41 was synthesized by the aforementioned procedure without adding the metal salt.

2.3. Incorporation of naphthalimide derivatives into MCM-41 by impregnation method

The various MCM-41 were added to 5 ml dye solution (10^{-4} mol/l, methanol/water = 4:1). After stirred for 3 h at ambient temperature, the solid was filtered and rinsed thoroughly with methanol and distilled water till the filtrate was clear. Then the samples were dried at 353 K for characterization.

3. Charaterization

Powder X-ray diffraction (XRD) measurement was carried out with a Rigaku D/MAX-2550 diffractometer using Cu Kα radiation within the scattering angel 2θ range of 0.8–10°, typically run at a voltage of 40 kV and current of 100 mA. The UV–vis absorption spectra were recorded with Varian Cary 500. The fluorescence spectra were obtained on a Cary Eclipse fluorescence photospectrometer. ^{1}H NMR spectra were measured on a Brücker AM500 spectrometer. The decay curves were recorded on Edinburgh FLS920. The infrared spectroscopic was made using a Nicolet 380 spectrometer from Thermo Electron (KBr pellet technique). All measurements were carried out at ambient temperature.

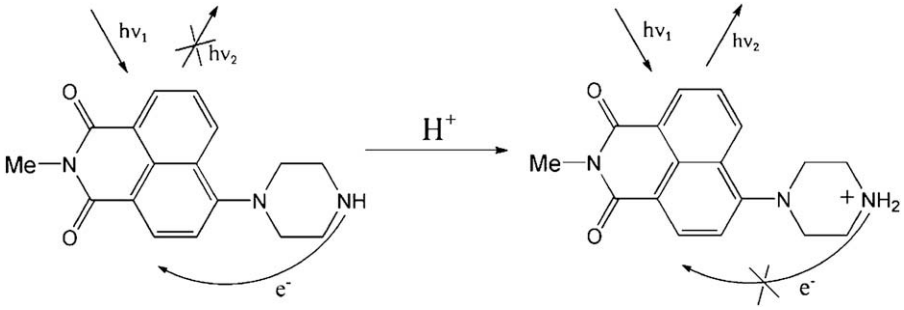

Scheme 1. Photoinduced electron transfer path in PMN.

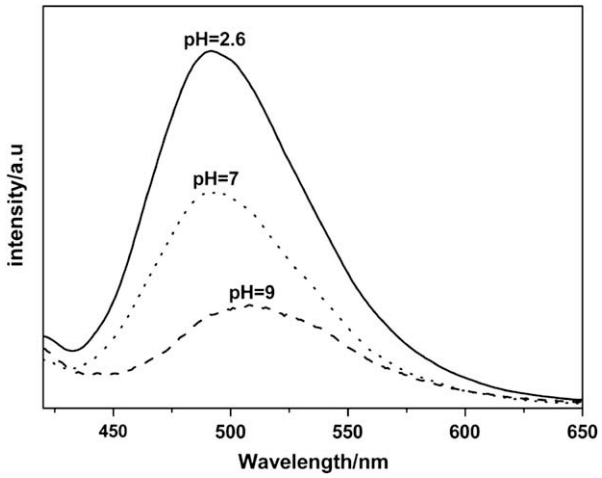

Fig. 4. Fluorescent emission spectra of PMN in Si-MCM-41 at different pH values (pH = 2.6, 7, 9).

4. Results and discussions

The XRD patterns shown in Fig. 1 indicated that all these mesoporous materials have three typical reflections of MCM-41, corresponding to the (100), (110) and (210) reflections. All the reflections are indexed based on hexagonal symmetry.

The maximum absorption peak position (397 nm) and the shape of PMN in MCM-41 is so similar to that in solution (shown in Fig. 2), which indicates that the dye molecules exist in monomer form in MCM-41 due to high surface area. In Fig. 3, the emission band of PMN/MCM-41 is not symmetrical and tails to longer wavelength. The result corroborates the characterization of the bands as combination bands with significant contributions from intramolecular charge transfer (ICT) normal (planar) mode transition as well as other accessible conformers [14]. The maximum emission peak of PMN molecules in Si-MCM-41 is blue-shifted to 493 nm, compared with that in methanol/water (v/v = 4:1) solution (520 nm). The large blue-shift (27 nm) of the emission band of PMN molecules in MCM-41 host in contrast with that in solution reflects that the local environment of MCM-41 has less polarity than methanol–water mixed solvent. On the other hand, there are carbonyl groups in PMN molecules, which will form hydrogen bonds with silanol groups of internal surface of MCM-41. The interaction of the carbonyl groups with the silanol groups can be verified by the fact that they could not physically absorb in the silylated MCM-41 due to the loss of hydrogen bond, when the silylated MCM-41 was added to the dye solution. The rigidly held PMN molecules which prevent the exited states from relaxing could cause the pronounced shift [15]. Because there is no organic solvent around the dye molecule in molecular sieve, the lack of solvation of the excited state will also lead to destabilization and increasing energy between the ground state and the excited state. Otherwise, if solvent relaxation is slow compared with excited-state lifetime, as in a rigid glass, then in general, the optimum solute–solvent configuration cannot be realized and an emission blue-shift results [16]. Hence we can deduce that the PMN molecules cannot attain the optimum configuration in such confined environment and result in the spectral shift. The fluorescence emission of PMN molecules in MCM-41 decreases drastically compared with that in organic solvent. The result can be attributed to the host–guest interaction which causes non-radiated energy transition of the dye molecules. Moreover the width of the hybrid material's emission band suggests a greater dephasing of excitonic energy than that for PMN molecules in solution [17].

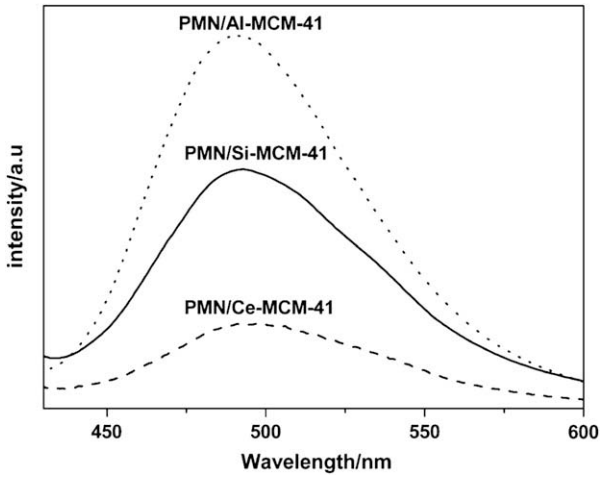

Fig. 5. Fluorescent emission spectra of PMN in Si-MCM-41, Ce-MCM-41, Al-MCM-41.

As shown in Scheme 1, the fluorescence emission of the fluorophore (*N*-methyl-1,8-naphthalimide) is quenched via photoinduced electron transfer (PET) within PMN molecule. This PET process occurs from the donor (piperadine) to the fluorophore (*N*-methyl-1,8-naphthalimide). When the PET process is stopped by protonation, the fluorescence of the fluorophore will be recovered. We speculated that the emission intensity of PMN molecules in MCM-41 changes with different pH values. So we design the

Table 1
The fluorescence data of PMN in different hosts.

Host	τ_1 (ns)	τ_2 (ns)	χ^2
Methanol/water	7.33	–	1.091
Si-MCM-41	8.40	1.94	1.136
Ce-MCM-41	7.63	2.89	1.096
Al-MCM-41	12.84	5.58	1.038

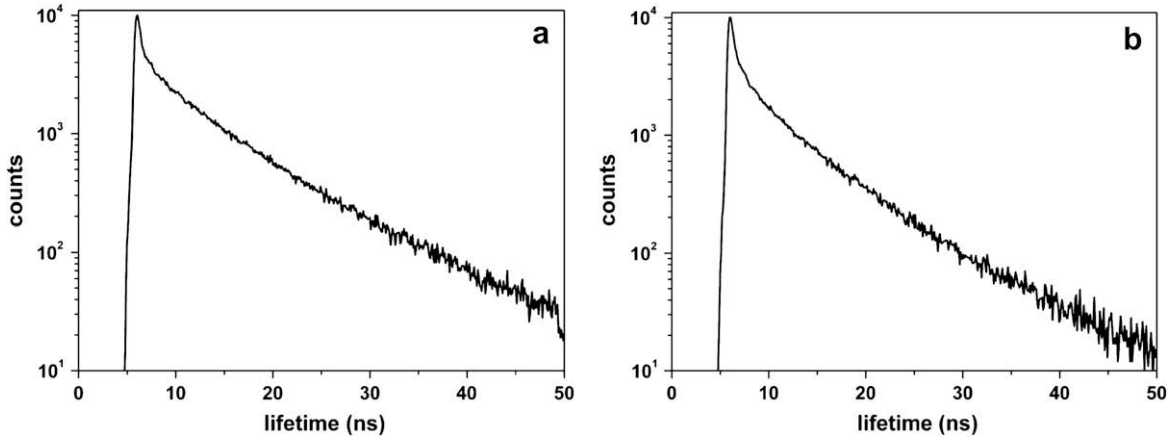

Fig. 6. Fluorescence decay curves for PMN in Al-MCM-41 (a, Si/Al = 100) and Ce-MCM-41 (b, Si/Ce = 100).

experiment in such a way that the dye encapsulated MCM-41 is added into aqueous solution at different pH values and investigate its fluorescent emission intensity. The result shown in Fig. 4 validates our deduction that the maximum emission intensity of PMN molecules in MCM-41 under acid condition increases 3.45 times than that under basic condition. The fluorescence enhancement effect in MCM-41 by hindering the PET process is not distinct as compared with that in solution [13]. The explanation can be rationalized that hydroxide ions or protons are difficult to diffuse into the pore structure of MCM-41 and bind with terminal N atom of PMN molecules in the deep location. With the increasing pH value, the emission peak is red-shifted (Fig. 4). Gan et al. also found the same phenomenon in solution [18].

Continuing with Fig. 5, it is observed that the emission peaks of PMN in Si-MCM-41, Al-MCM-41, Ce-MCM-41 are almost at the same position, but have remarkably different intensity. To our knowledge, metal ions introduced into MCM-41 will quench the fluorescence of encapsulated dye molecules. Because the occurrences of the high charge transfer efficiency between dye molecules and metal-doped mesoporous material can quench the fluorescence of dyes. But in our researching system, it can only be observed in the PMN/Ce-MCM-41 system. The fluorescence of PMN in Al-MCM-41 increases by 54.2% than that in Si-MCM-41. This unexpected result can be attributed to the increasing anchored amount and the acid sites in Al-MCM-41. Besides the silanol sites, the metal ion sites can also easily absorb such neutral dye molecules. The acid sites presented in Al-MCM-41 can afford protons to prevent PET process within PMN molecule and recover the fluorescence. Maybe the unexpected fluorescence enhancement can also be explained that the protonated PMN molecules cannot approach the Al^{3+} sites nearly and decrease the electron transfer efficiency owing to electrostatic repulsion. This unusual result has been supported by the fluorescence decay data which is depicted below.

Table 1 shows that all fluorescence decay curves of PMN in mesoporous materials exhibit biexponential decay curves, compared with the monoexponential decay curve of PMN in solution. The biexponential decay curves have a longer lifetime (τ_1) and a shorter one (τ_2). It indicates that the dye molecules absorb on two types of existing site. As shown in the fluorescence decay data of PMN in metal-doped MCM-41 (Fig. 6), the long lifetime (τ_1) probably represents the dye molecules absorb on the silanol sites and the short one (τ_2) represents the dye molecules absorb on the isolated metal ion sites. For the short lifetime form, the PMN molecules are fixed on the isolated metal ion sites and high energy transition efficiency can occur between guests and hosts. As shown in Fig. 6, the lifetime of PMN in Al-MCM-41 is much longer than that in Ce-MCM-41. The explanations are listed below. (1) The acid sites in Al-MCM-41 can release protons and make the PMN molecules protonated. The protonated dye molecules cannot approach the metal ion sites in molecular sieve. The longer distance between dyes and hosts due to electrostatic repulsion decreases the charge transfer efficiency, so the short time (τ_2) in Al-MCM-41 is longer than that in Ce-MCM-41. (2) If the charge transfer in the dye molecules is accessible at dynamics, the relative stable excited state is required. The stable excited state can keep electron retain within PMN molecules. The PET process which occurs between the donor and the fluorophore win the advantage over the charge transfer process from the PMN molecules to the metal ion sites. The electrons incline to be transferred to the acceptor within the dye molecules, not the metal ion sites of host. The prolonged time constant (τ_1) in Al-MCM-41 approves this speculation.

5. Conclusions

The naphthalimide derivative is firstly encapsulated into the channels of mesoporous materials. The absorption spectra show that PMN molecules existed in monomer form. The fluorescence emission of PMN in MCM-41 shifts to short wavelength compared with that in solution. Owing to the photoinduced electron transfer process, the emission intensity of PMN molecules in MCM-41 increases with pH value decreasing. The emission intensity of PMN in Al-MCM-41 is abnormally larger than that in Si-MCM-41 and the fluorescent lifetime of PMN in Al-MCM-41 is prolonged. The result indicates that the electrostatic repulsion between the pronated PMN molecules and Al-MCM-41 will cause the decreasing electron transfer efficiency from guest to host.

Acknowledgements

This work has been sponsored by National Basic Research of China (973 Program 2004CB719500), National Nature Science Foundation of China (20773039), the Research Fund for the Doctoral Program of Higher Education (20070251006) and the Ministry of Science and Technology of China (2006AA06Z379, 2007AA05Z303, 2006DFA52710).

References

[1] MacCraith BD. Chem Anal 1998;150:195.
[2] Schomburg C, Rohlfing Y, Schulz-Ekloff G, Wark M, Wohrle D. J Mater Chem 2001;11:2014.
[3] Marlow F, McGehee MD, Zhao D, Chmelka BF, Stucky GD. Adv Mater 1999;11:632.
[4] Caro J, Finger G, Kornatowski J, RichterMendau J, Werner L, Zibrowius B. Adv Mater 1992;4:273.
[5] Mal NK, Fujiwara M, Tanaka Y. Nature 2003;421:350.

[6] Mal NK, Fujiwara M, Tanaka Y, Taguchi T, Matsukata M. Chem Mater 2003;15:3385.
[7] Yuliarto B, Honma I, Katsumura Y, Zhou HS. Sens Actuators B 2006;114:109.
[8] Laha SC, Mukherjee, Sainkar SR, Kumar R. J Catal 2002;207:213.
[9] Zhao WJ, Li DM, He B, Zhang JL, Huang JZ, Zhang LZ. Dyes Pigments 2005;64:265.
[10] Shao YF, Wang LZ, Zhang JL, Anpo M. J Photochem Photobiol A 2006;180:59.
[11] Saha S, Samanta A. J Phys Chem A 2002;106:4763.
[12] Grabtchev I, Chovelon JM. Dyes Pigments 2008;77:1.
[13] Gan JA, Chen KC, Tian H. J East China Univ Sci Technol 2001;27:217.
[14] Elbert JE, Paulsen S, Robison L, Elzey S, Klein K. J Photochem Photobiol A 2005;169:9.
[15] Incavo JA, Dutta PK. J Phys Chem 1990;94:3075.
[16] Andrews LJ. J Phys Chem 1979;83:3203.
[17] Xu W, Guo HG, Akins DL. J Phys Chem B 2001;105:7686.
[18] Gan JA, Chen KC, Chang CP, Tian H. Dyes Pigments 2003;57:21.